

## 16.4 A Flexible EEG Acquisition and Biomarker Extraction System Based on Thin-Film Electronics

Tiffany Moy, Liechao Huang, Warren Rieutort-Louis, Sigurd Wagner, James C. Sturm, Naveen Verma

Princeton University, Princeton, NJ

EEG is an important modality for many medical purposes. However, the low-amplitude of signals (10-to-100 $\mu$ V) and large number of channels (~20) raise numerous challenges, including electrode setup (correct placement, skin preparation, sanitation), patient comfort (number of channels, skin abrasion), and robust acquisition (electrode/wire motion artifacts, wire stray coupling). The recent emergence of low-cost, single-use, flexible, pre-gelled electrode arrays, as in Fig. 16.4.1, delivers significant advantages [1]. Today, these are passive, requiring connection to external readout electronics via a many-channel cable. We present the system in Fig. 16.4.1, having similar flexible form factor, but with the following enhancements: (1) embedded low-noise chopper-stabilized amplifiers using amorphous-silicon (a-Si) thin-film transistors (TFTs) compatible with flexible substrates (i.e. low-temperature-processed, <180°C); (2) compressive-sensing acquisition and multiplexing of >20 EEG channels onto a single interface using TFT scanning circuits, to substantially ease connection with an embedded IC; and (3) an algorithm whereby spectral-energy features, a generic EEG biomarker, are derived directly from the compressed signals (by a conventional CMOS IC). Seizure detection from the extracted features is demonstrated via analog replay of patient EEG through the system.

Previous instrumentation amplifiers using low-temperature-processed TFTs have focused on signals such as EMG [2], and do not achieve noise levels needed for EEG (which has significantly lower amplitude). Figure 16.4.2 shows the measured input-referred noise PSD of an a-Si amplifier, with biasing of 200 $\mu$ A. The band of interest for EEG (0-to-300Hz) is limited by 1/f noise, which can be high for low-temperature-processed TFTs due to high carrier-trap density in the semiconductor and semiconductor-dielectric interface [3]. Typically, 1/f noise is reduced by increasing device W and L. Though effective for TFTs, this worsens reliability, as shown in Fig. 16.4.2. Pinholes (associated with low-temperature-deposited gate dielectrics) cause the increasing TFT defect rate shown with W and L, limiting the extent to which sizing can address 1/f noise.

Instead, the instrumentation amplifier in Fig. 16.4.3 is demonstrated, based on chopper stabilization. The gain stage as well as input/output modulators are implemented using NFET a-Si TFTs. We demonstrate substantial reduction of 1/f noise despite the performance and power-efficiency limitations of TFTs. Regarding performance, the TFTs have max.  $f_T \approx 1$ MHz (measured), enabling up-modulation of signals beyond a 1/f corner of 5kHz (as in the biasing of Fig. 16.4.2 for white-noise floor of 140nV/ $\sqrt$ Hz). Regarding power-efficiency, the metric of interest for instrumentation amplifiers is transconductance efficiency ( $g_m/I_D$ ). Generally, circuit functions are implemented in Si CMOS ICs wherever possible, due to the orders-of-magnitude superior transistor parameters (mobility, extrinsic capacitances). However, for robust acquisition, TFT-implemented instrumentation: (1) is necessary, to be close to distributed sensors; and (2) achieves reasonable levels of transconductance efficiency, since both  $g_m$  and  $I_D$  are similarly affected by the transistor parameters. As shown in Fig. 16.4.3 (based on a-Si TFT measurements and 130nm Si transistor simulations),  $g_m/I_D$  exhibits relationship with  $f_T$ , as the gate-overdrive is varied. Thus, the up-modulation needed in chopper stabilization affects power efficiency somewhat; but, as an example, for 5kHz chopping frequency, requiring TFT  $f_T$  greater than ~50kHz,  $g_m/I_D$  within a factor of 20 of Si transistors is possible. Further improvement is expected as we move to other TFT technologies (e.g. metal oxides).

The implementation employs a 5kHz digital chopping signal CHOP distributed to all amplifiers, from a conventional CMOS IC through a TFT level converter [4]. The TFT sizes, stage biasing currents, and load resistances are as shown in Fig. 16.4.3, yielding a stage gain >10. Following the output modulator, a single-pole passive low-pass filter with cut-off frequency of 500Hz is implemented.

Following amplification, signals are multiplexed for subsequent readout and processing by a conventional CMOS IC. This reduces the number of bonds to the IC, which significantly benefits assembly cost and reliability on flexible substrates. Multiplexing is achieved using the TFT scanning circuit presented in [4], whereby channels are sequentially selected by enabling analog TFT switches. As is typical, the speed of the TFT scanning circuit is limited to ~10kHz. Given their frequency content following single-pole filtering, Nyquist sampling would limit the number

of channels in the system to <5. However, as EEG is known to be sparse in the Gabor basis, the scanning implementation shown in Fig. 16.4.4 is used, employing an architecture that exploits compressive sensing [5]. The architecture consists of modulation (using TFT switches) with a 500Hz pseudorandom  $\pm 1$  digital chipping sequence CHIP (distributed to all channels from a conventional CMOS IC through a TFT level converter [4]), followed by low-pass filtering with cutoff frequency <0.03Hz, to approximate integration. For demonstration, patient EEG from the CHB-MIT dataset, sampled at 256Hz, is replayed through the system by appropriately scaling the output of a 16b DAC. Figure 16.4.4 shows waveforms reconstructed from samples acquired by the system at 1-to-8 $\times$  below the Nyquist rate.

Though the original EEG can be obtained in this way, full sparse reconstruction is computationally intensive. In many applications, extracting spectral-energy features is the primary interest. We present an approach, extending our previous algorithmic work [6], to obtain these efficiently from the compressed signals. As shown in Fig. 16.4.5, using the N-point vector  $\vec{x}$  to represent EEG time samples in an epoch, a band-pass filtered signal  $\vec{y}$  is obtained by multiplication with a matrix:  $\vec{y} = H\vec{x}$ . The M-point compressed EEG  $\Phi\vec{x}$  provides an underdetermined system of linear equations for recovering the underlying sparse signal when  $M < N$  (i.e.  $\Phi$  is the  $M \times N$  compressive-sensing measurement matrix corresponding to the analog scanning system). Nonetheless, the error from linear estimation is tolerable as: (1) the underlying sparse signal is in the Gabor domain, and so the error, affecting all elements, will in many cases be attenuated following band-pass filtering; and (2) since our interest is ultimately in the energy given by  $\|\vec{y}\|_2^2$ , the error accumulated over all elements has diminished variance relative to the energy. In fact, in addition to linear estimation, further energy saving is possible by seeking random measurements of  $\vec{y}$  rather than  $\vec{y}$  itself. Since  $\vec{y}$  from band-pass filtering is at least as sparse as  $\vec{x}$  in the Gabor basis, a K-row compressive matrix  $\Theta$  (with  $K \leq M$ ) whose elements are drawn from a Gaussian distribution, will present the property  $\alpha\|\vec{y}\|_2^2 \approx \|\Theta\vec{y}\|_2^2$ , with some bound error (restricted isometry property). Thus, the desired spectral energy  $\|\vec{y}\|_2^2$  can be estimated from  $\Theta\vec{y}$ . This allows us to solve for a compressed  $K \times M$  transform  $\hat{H}$  such that  $H\Phi\vec{x} = \Theta\hat{H}\vec{x}$  (e.g. by finding a minimum-norm solution to  $\Theta H - H\Phi$ ). For illustration, Fig. 16.4.5 compares estimates from 20 epochs (of 2sec length) for an EEG channel (10/10 non-/seizure) after filtering (center at 0Hz, bandwidth of 3Hz). A seizure detector is implemented by feeding 8 such features (filter centers 0-21Hz) from 7 EEG channels to an SVM classifier. True-pos./true-neg./error rates (TP/TN/Err) vs. compression are shown in Fig. 16.4.5, using 4950/100 non-/seizure epochs of EEG randomly sampled from one patient in the CHB-MIT dataset (replayed via a 16b DAC); direct classification results TP/TN/Err are shown, since sampling prevents mapping to latency/sensitivity/false-alarms.

The EEG acquisition system on flex is fabricated with a-Si TFTs processed in house at temperatures <180°C (Fig. 16.4.7). Figure 16.4.6 presents a measurement summary. Chopper stabilization reduces input-referred noise in the band of interest to 230nV/ $\sqrt$ Hz, and increases the CMRR to above 40dB (limited by mismatch in TFTs, expected to improve with process refinement). Successful EEG acquisition is shown, by recording  $\alpha$  waves from a standard Ag/AgCl electrode positioned at the occipital location (evoked by 10sec periods of closing/opening the eyes). The power drawn by the amplifier is 11mW from a 55V supply.

### Acknowledgements:

Funding provided by NSF (grant ECCS-1202168) and Systems on Nanoscale Information fabriCs (SONIC), one of six STARnet Centers, sponsored by MARCO and DARPA.

### References:

- [1] Hydrodot, Inc. StatNet. [Online]. Available: <http://hydrodot.net/>.
- [2] H. Fuketa et al., "1 $\mu$ m-Thickness Ultra-Flexible and High Electrode-Density Surface Electromyogram Measurement Sheet with 2V Organic Transistors for Prosthetic Hand Control," *IEEE Trans. Biomedical Circuits and Systems*, vol. 8, no. 6, pp. 824-833, Dec. 2014.
- [3] W. Rieutort-Louis et al., "Representative Flicker Noise Measurements for Low-Temperature Amorphous Silicon, Organic, and Zinc Oxide Thin-film Transistors," *Int'l Thin-Film Transistor Conf.*, Feb. 2015.
- [4] T. Moy et al., "Thin-Film Circuits for Scalable Interfacing Between Large-Area Electronics and CMOS ICs," *Device Research Conf.*, pp. 271, June 2014.
- [5] S. Kirolos et al., "Analog-to-Information Conversion via Random Demodulation," *IEEE Dallas Circuits and Systems Work.*, pp. 71-74, Oct. 2006.
- [6] M. Shoab, N.K. Jha, N. Verma, "Signal Processing With Direct Computations on Compressively Sensed Data," *IEEE Trans. VLSI Systems*, vol. 23, no.1, pp. 30-43, Jan. 2015.

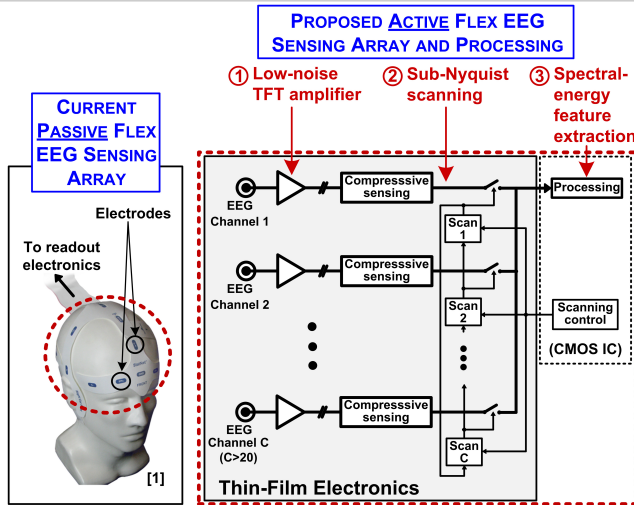


Figure 16.4.1: System architecture enhancing current passive flex EEG electrode arrays [1], by introducing TFT amplifiers and acquisition circuits on flex, and a spectral feature-extraction algorithm.

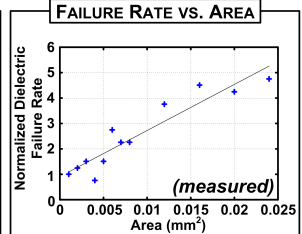
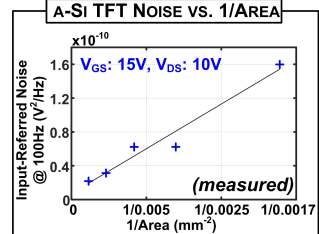
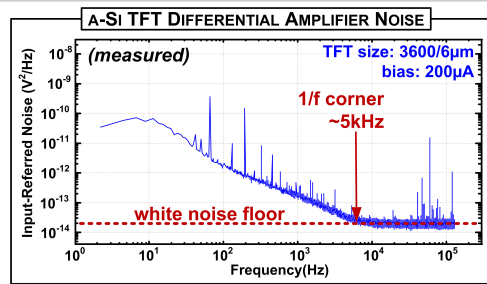


Figure 16.4.2: Measured 1/f-limited noise PSD of an a-Si TFT amplifier, and TFT W, L sizing effect on 1/f noise and gate dielectric reliability.

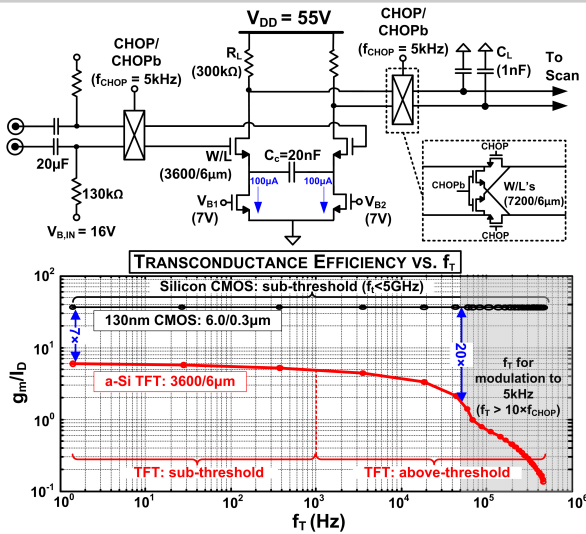


Figure 16.4.3: Chopper-stabilized a-Si TFT low-noise amplifier and  $g_m/I_D$  analysis, showing  $f_t$  required for up-modulation.

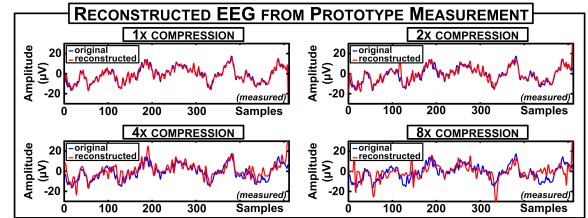
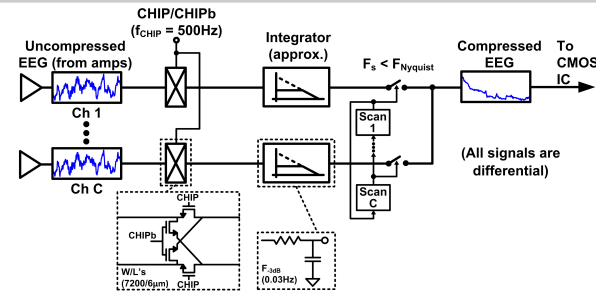


Figure 16.4.4: TFT-based compressive-sensing scanning acquisition, and reconstructed waveforms measured by analog replay of EEG from CHB-MIT dataset through the prototype.

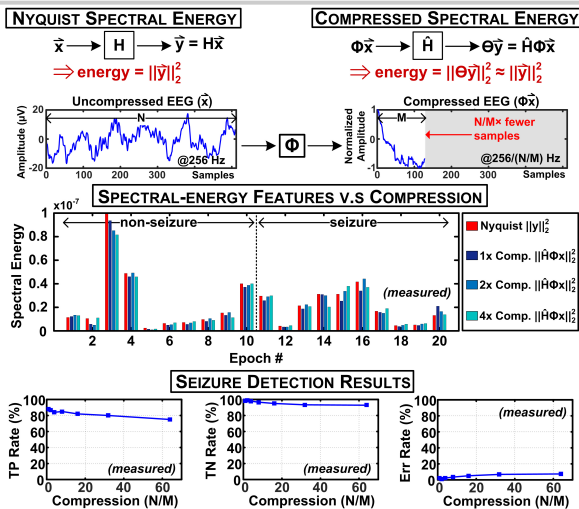


Figure 16.4.5: Spectral feature extraction from compressed signals (top); comparison of derived features from different compression levels (middle); and seizure detection results (bottom).

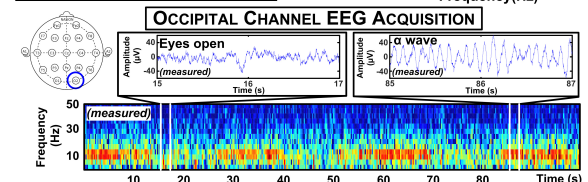
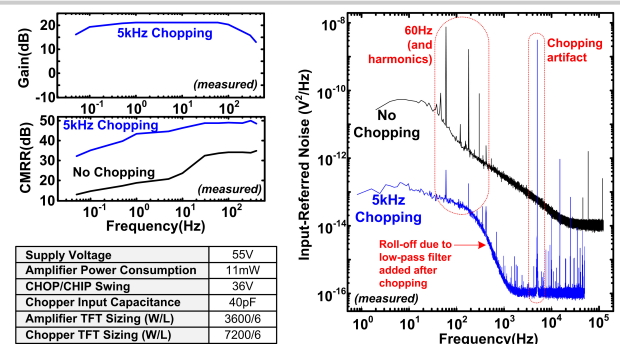


Figure 16.4.6: Measured performance summary and EEG acquisition of  $\alpha$  wave from subject using Ag/AgCl electrodes.

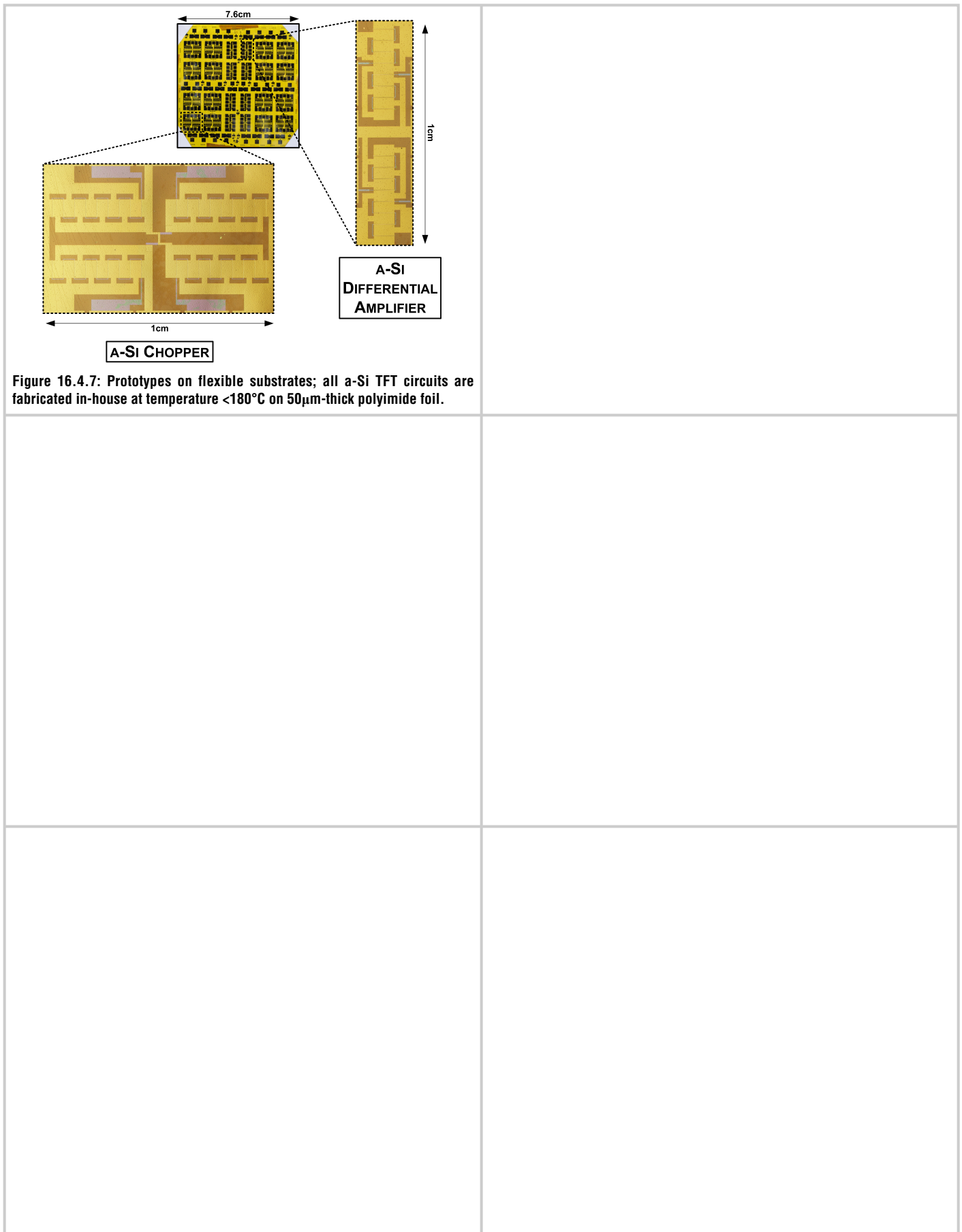


Figure 16.4.7: Prototypes on flexible substrates; all a-Si TFT circuits are fabricated in-house at temperature  $<180^{\circ}\text{C}$  on  $50\mu\text{m}$ -thick polyimide foil.